U.S. Army Research Laboratory

SUMMER RESEARCH TECHNICAL REPORT

Tunable, Highly Ordered TiO$_2$ Nanotube Arrays on Indium Tin Oxide Coated PET for Flexible Bio-sensitized Solar Cells

JOSHUA J. MARTIN, UNIVERSITY OF DELAWARE
MENTORS: DR. SHASHI KARNA AND DR. MARK GRIEP
U.S. ARMY RESEARCH LABORATORY, WMRD, RDRL-WMM-A
ABERDEEN PROVING GROUND, MARYLAND

Report Documentation Page

1. REPORT DATE **AUG 2011**	2. REPORT TYPE	3. DATES COVERED **00-00-2011 to 00-00-2011**

4. TITLE AND SUBTITLE	5a. CONTRACT NUMBER
Tunable, Highly Ordered TiO2 Nanotube Arrays On Indium Tin Oxide Coated PET For Flexible Bio-sensitized Solar Cells	5b. GRANT NUMBER
	5c. PROGRAM ELEMENT NUMBER

6. AUTHOR(S)	5d. PROJECT NUMBER
	5e. TASK NUMBER
	5f. WORK UNIT NUMBER

7. PERFORMING ORGANIZATION NAME(S) AND ADDRESS(ES) **U. S. Army Research Laboratory,Aberdeen Proving Ground,MD,21005**	8. PERFORMING ORGANIZATION REPORT NUMBER

9. SPONSORING/MONITORING AGENCY NAME(S) AND ADDRESS(ES)	10. SPONSOR/MONITOR'S ACRONYM(S)
	11. SPONSOR/MONITOR'S REPORT NUMBER(S)

12. DISTRIBUTION/AVAILABILITY STATEMENT
Approved for public release; distribution unlimited

13. SUPPLEMENTARY NOTES
See also ADA548876

14. ABSTRACT

Highly ordered, free-standing titanium dioxide (TiO2) nanotube (TNT) arrays have been of intense interest in the alternative energies field in recent years due to their barrier-free electron conduction pathway versus TiO2 nanoparticles in dye sensitized solar cell (DSSC) designs. TNT arrays prepared by electrochemical anodization of titanium (Ti) foils and combined with a transparent, indium tin dioxide coated polyethylene terephthalate (PET) film are attractive candidates for efficient, flexible DSSCs. Flexible solar cells offer great benefits because of the potential for low-cost, roll-to-roll production and the increase in applications due to superior robustness. This approach uses a two-step anodization procedure coupled with implementation of a rapid inert gas dehydration and ultrasonic agitation detachment method. By controlling the reaction conditions during anodization (voltage, duration, and concentration), TNT arrays with specific morphology, lengths, and diameters can be tailored to satisfy a particular application such as incorporating specialized protein dyes, in particular, bacteriorhodopsin (bR). The free-standing arrays, comprised of hexagonally closed-packed and regularly ordered TNT membranes, have been synthesized and detached from the original Ti substrate. Once the TiO2 sol-gel is created, the free-standing arrays will be attached to the flexible PET film for improved photovoltaic properties and overall performance.

15. SUBJECT TERMS

16. SECURITY CLASSIFICATION OF:			17. LIMITATION OF ABSTRACT	18. NUMBER OF PAGES	19a. NAME OF RESPONSIBLE PERSON
a. REPORT **unclassified**	b. ABSTRACT **unclassified**	c. THIS PAGE **unclassified**	**Same as Report (SAR)**	**18**	

Contents

List of Figures

Abstract

Highly ordered, free-standing titanium dioxide (TiO_2) nanotube (TNT) arrays have been of intense interest in the alternative energies field in recent years due to their barrier-free electron conduction pathway versus TiO_2 nanoparticles in dye sensitized solar cell (DSSC) designs. TNT arrays prepared by electrochemical anodization of titanium (Ti) foils and combined with a transparent, indium tin dioxide coated polyethylene terephthalate (PET) film are attractive candidates for efficient, flexible DSSCs. Flexible solar cells offer great benefits because of the potential for low-cost, roll-to-roll production and the increase in applications due to superior robustness. This approach uses a two-step anodization procedure coupled with implementation of a rapid inert gas dehydration and ultrasonic agitation detachment method. By controlling the reaction conditions during anodization (voltage, duration, and concentration), TNT arrays with specific morphology, lengths, and diameters can be tailored to satisfy a particular application such as incorporating specialized protein dyes, in particular, bacteriorhodopsin (bR). The free-standing arrays, comprised of hexagonally closed-packed and regularly ordered TNT membranes, have been synthesized and detached from the original Ti substrate. Once the TiO_2 sol-gel is created, the free-standing arrays will be attached to the flexible PET film for improved photovoltaic properties and overall performance.

Acknowledgments

Student Bio

I am currently a rising senior at the University of Delaware studying mechanical engineering with a biomedical engineering minor. I am a member of the Society for the Advancement of Material and Process Engineering (SAMPE) and Engineers Without Borders Club on campus, as well as the President of the Rock Climbing Club. This is my first research period at the U.S. Army Research Lab. After graduating from UD, I plan on pursuing my interest in renewable energy. After a few years, I intend on applying everything I have learned to a term with the Peace Corps.

1. Background Information

Soldiers and vehicles are particularly constrained by a dependence on bulky batteries to meet their power needs. Future force Soldiers will be equipped with a wide array of technology, essentially all of which requiring electrical power for operation. Integrating solar harvesting capabilities with future equipment would relieve the burden of batteries and increase overall performance of Soldiers, as well as provide relief toward the need for renewable energy sources. While modern silicon (Si) cells are costly to produce and adversely affect mobility, dye-sensitized solar cells are providing very advantageous properties. These systems are prospectively capable of achieving higher efficiencies, more attractive costs, and lower environmental impact, and are more easily manufactured than current Si solutions. Dye-sensitized titanium oxide (TiO_2) platforms do not require expensive semi-conductor substrates, nor do they require highly complex processing steps, making roll-to-roll production possible (*1*). Most importantly, they can be geared to be highly robust and flexible. These attributes qualify dye-sensitized solar cells (DSSCs) as a chief candidate for future solar energy harvesting systems, and will facilitate a successful entry to the Si-dominated market.

The objective of the research presented in this paper is to develop and optimize TiO_2 nanotubes for a flexible, dye-sensitized solar cell. Particular focus will go into producing highly ordered nanotube arrays with a tunable pore diameter to compensate for a bacteriorhodopsin (bR) dye, thus increasing the organic nature of the cell. Removal of the nanotube arrays from the Ti substrate using methanol wetting and N_2 blowing will make it possible to make a front-side illuminated solar cell, while replacing the conducting substrate with indium tin dioxide-coated PET increases the flexibility and conductivity.

1.1 DSSC Overview

The classic DSSC is composed of a layer of nanocrystalline TiO_2 particles on a conducting substrate, a platinum counter electrode, an electrolyte, and an adsorbed ruthenium (Ru)-dye as a sensitizer (*2*). In contrast to conventional Si systems, where the semiconductor assumes both the light absorption and charge carrier transport, the two functions are separated here (*3*). The operating principle is demonstrated in figure 1. On the surface of the TiO_2 is an adsorbed dye, attached by specific functional groups, which serves as a light absorber and photon-to-electron converter. A key requirement for the dye is that the lowest unoccupied molecular orbital
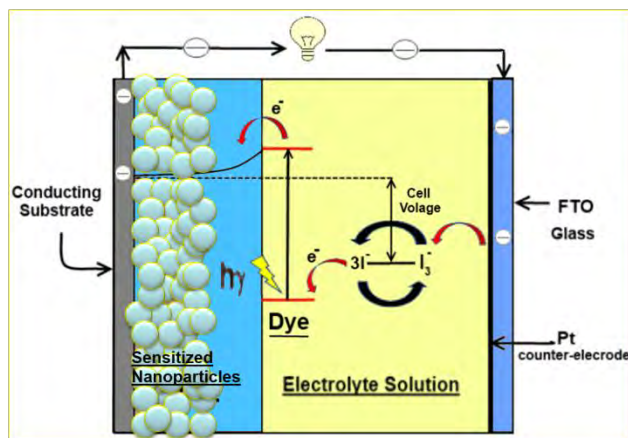
Figure 1. Principle of a DSSC.

(LUMO) of the dye molecule is energetically positioned slightly higher than the conduction band of TiO_2. Under the illumination of sunlight, highest occupied molecular orbital (HOMO)–LUMO transitions in the dye occur. Photoexcitation of the dye leads to rapid injection of electrons into the TiO_2. These electrons are then collected to power an external load. For typically used Ru dyes, the electron injection from the dye sensitizer to the conduction band of TiO_2 occurs through a metal-to-ligand charge transfer (MLCT) pathway (*4*). Electron donation from the redox couple in the electrolyte, usually an ionic liquid containing an I_3^-/I system, regenerates the oxidized dye and returns it to its original state. The tri-iodide ions formed in the dye regeneration process diffuse through the liquid phase to the cathode, where they are reduced back to iodide ions to complete the cycle (*5*). The efficiency of collection of the photoinjected electrons, which is a critical factor in device performance, is determined by competition between electron transport to the anode and electron transfer to the I_3^- ions electrolyte. Research using such constructions has achieved light-to-electricity conversion efficiencies of 11% (*6*).

While this demonstrates much prospect, the electron transport time in TiO_2 nanoparticles is relatively slow when compared to the rate of de-excitation of the dye and the regeneration time constant of the dye (*7*). Electron flow is slowed down due to defects, surface states, grain boundaries, and other sites of electron trapping within the nanoparticles. These factors enhance recombination and adversely affect electron transfer (*8*). In other words, the majority of excited electrons recombine with the dye before they can be collected to power a load. To minimize this effect, recent research has explored the use of more organized TiO_2 structures such as nanotubes.

TiO_2 nanotubes have a highly ordered structure with vertical pore geometry, which appears to be very suitable for the fabrication of solid-state junction cells (*9*). This is due mainly to the 1-D conductive path of nanotubes vs. the 3-D unsystematic walk network and grain boundary effects of randomly associated nanoparticles, displayed in figure 2. It has been reported that compared to conventional TiO_2 nanoparticle films of the same thickness, nanotube arrays give enhanced light scattering and improved collection efficiencies (*10*). Therefore, this study will be using the TiO_2 nanotube platform displayed in figure 3.
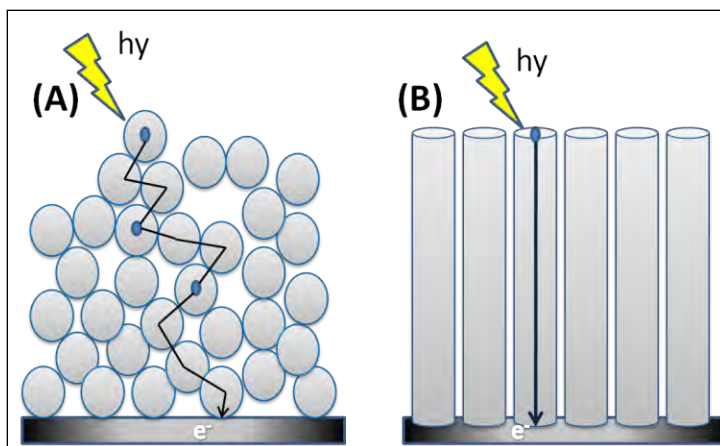
Figure 2. (a) Random electron walk in nanoparticles. (b) 1-D electron transport in nanotubes.
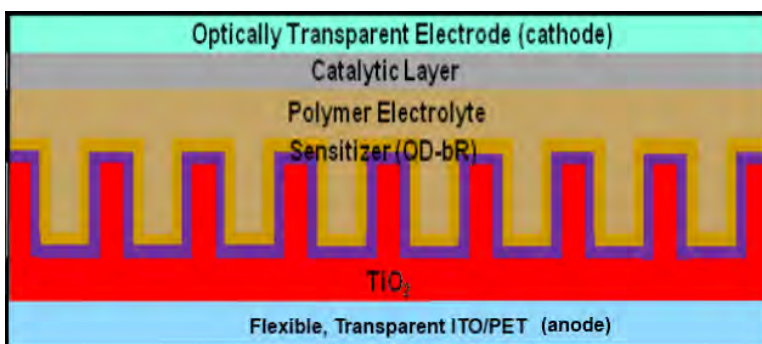

Figure 3. Proposed Concept design.

1.2 Critical Factors for Efficiency

It has been established that the conversion efficiency of DSSCs is mainly governed by molar absorption coefficient and HOMO-LUMO levels of the dye, the effective surface area of the electrodes available for dye anchoring, the transport kinetics of electrons to the substrate, the efficiency of dye regeneration via a redox couple, and the losses arising from recombination and back reactions of injected charge carriers (*11*). Many papers exist with the goal of optimizing key components of DSSCs, such as the TiO_2 structures, the dye, and the electrolyte used. However, it is beyond the scope of this paper to go into a detailed review of each topic. Critical optimization factors pertaining to the TiO_2 arrays will be outlined, with a particular focus in maximizing pore diameter to accommodate for the bR dye.

The performance of TiO_2 nanotube arrays in a DSSC as an efficient semi-conductor and electron recipient is directly related to several factors: morphology, crystallinity, and geometry (*2*). Many studies have been conducted in order to control the dimensions of TNT arrays via anodic oxidation (anodization). It has been shown that uniform TiO_2 nanotube arrays with various lengths, diameters, and wall thicknesses can be fabricated in fluoride containing solutions (HF

197

and NH_4F) by tailoring the electrochemical conditions (anodization voltage, fluoride concentration, anodization time, and temperature) (*12–14*).

1.2.1 Growth of TiO$_2$ Nanotube Arrays

The simple electrochemical process of anodizing Ti foils, displayed in figure 4, to produce TNTs can be accomplished using a two- (or three-) electrode system, with Ti-foil as the working electrode (+), a counter electrode such as platinum (Pt) (−), and a voltage source. Nanotube formation in fluoride-ion-bearing electrolytes occurs due to three simultaneously occurring processes: the field assisted oxidation of Ti metal to form TiO_2, the field-assisted dissolution of Ti metal ions in the electrolyte, and the chemical dissolution of Ti and TiO_2 due to etching by fluoride ions (which is substantially enhanced by fluoride ions) (*16*). A thin dioxide film develops at the Ti/electrolyte interface due to the following chemical reaction (*10*):

$$Ti + 2H_2O \rightarrow TiO_2 + 4H^+ - 4e^-. \tag{1}$$

As this oxidation occurs, one can note that the current measured will reduce as time goes on. This is due to the increase in resistance provided by the oxide. As the oxygen ions (O^{2-}) are transported from the solution to the Ti, titanium ions (Ti^{4+}) transported from the titanium to the electrolyte interface are dissolved into the solution. A simultaneous reaction occurs at the TiO_2/electrolyte interface, forming soluble fluoride complexes. These create pits at the surface according to the following reaction (*10*):

$$TiO_2 + 6F^- \rightarrow TiF_6{}^{2-}. \tag{2}$$

These complexes dissolve and form pits on the surface of the newly formed TiO_2. As anodization time increases, all three processes continuously increase the depth of the pores (pits) and, therefore, produce highly ordered nanotubes (*19, 20*).
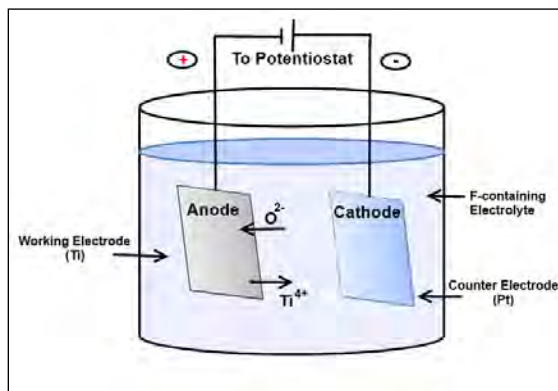

Figure 4. Anodization set up.

1.2.2 Length, Diameter, and Pore Size

Certain geometrical parameters of the nanotube arrays have a large effect on performance. It has also been found that by controlling the anodization setting, these parameters can be fairly

tunable. Length, diameter, and pore size (inner diameter) are largely influenced by anodization time, voltage, and NH_4F concentration (*15*). Increasing the overall length of the array allows for more surface area, resulting in more attached dye. The easiest way to modify the length of the array is to increase the anodization time. Due to the higher number of dye molecules that can attach to the increased length of the tubes, increasing thickness leads to an increase in the short circuit photocurrent. It is important to note that although the short circuit current is increased with tube length, so is the chance of recombination and electron trapping. It is reported that when the TNT length is significantly more than 20 μm, the diffusion length of the electron becomes shorter than the length of the TNT (*17*). Hence, the photovoltaic performance shows an initial increase and following decrease with the increasing TiO_2 nanotube length. The same study was able to achieve an outstanding conversion efficiency (Ŋ) of 8.07% using a 20.8 μm nanotube array with an open-circuit voltage (V_{OC}) of 0.814 V, a short-circuit current (J_{SC}) of 15.46 mA cm^{-2}, and a fill factor (FF) of 64.1%. This agrees with other studies that report the maximum internal conversion efficiency is achieved for tubes of a length of approximately 20 μm (*2*).

In order to further modify the dye "absorbing" capabilities of the nanotubes, diameter and pore size are very important. These factors are critical depending on certain situations. In order to take full advantage of nanotubes having both inner and outer walls, the dye being used must be able to fit inside of the inner diameter. According to Schmuki's studies (*9*), the diameter of the tubes can be adjusted by the anodization voltage. In addition, modifying the concentration of the electrolyte used during anodization further modifies the pore diameter and wall thickness. This occurs due to the increase in the dissolution rate, which increases due to a higher amount of F^- ions within the electrolyte solution, leading to an increase of the inner diameter—thus reducing wall thickness and increasing the pore size (*10*).

1.2.3 Crystalline Structure

The crystal structure of TiO_2 tube walls is a significant factor that affects the electronic properties of the array. When anodically formed, the TiO_2 arrays are initially in an amorphous state. Due to a large amount of defects, impurities, and other recombination sites, the amorphous TiO_2 has hardly any conversion efficiency (*11*). In order to harness the maximum potential of the TNT array, the nanotubes must be annealed to a crystallite form.

When annealed at temperatures between 300 and 500 °C for about 3 h, the anatase crystalline form of TiO_2 can be obtained. At higher temperatures—550 °C and above—rutile-based TiO_2 will begin to develop. In addition to annealing temperature, the ramping speed has an effect on solar cell performance (*2*). High ramping speeds (>30 °C/min) can adversely affect performance. Furthermore, annealing for longer periods of time increases crystallinity. Little attention has been paid to the rutile form of TiO_2, although it is used as a base in most paints due to its light-scattering ability. The anatase form of TiO_2 is perceived as more active than rutile because of its surface chemistry and potentially higher conduction-band energy (*18*). Rutile films consist of homogenously distributed rod-shaped particles. These particles show no preferred orientation

and, therefore, have a much smaller packing density compared to anatase-based particles. The smaller packing density results in a smaller particle connectivity. In other words, electrons move slower through rutile-based TiO_2 than in anatase-based. In addition, anatase arrays have a larger surface area per unit volume (about 25%); this allows for more dye to be absorbed. As a result, anatase structures can achieve a 30% higher J_{SC} than rutile. Maintaining a pure anatase TiO_2 nanostructure is essential for achieving a high efficiency DSSC using nanotubes.

2.   Experiment/Calculations

Highly ordered free-standing TiO_2 nanotube arrays were prepared using a two-step anodization process. Ti foils (99.7%, 0.25 μm) were purchased from Sigma-Aldrich and electrochemically anodized in a standard two-electrode cell using a Platinum counter-electrode and an Agilent E3649A DC power supply (figure A-1). The electrodes were kept at a fixed distance of 1.5 cm. The foils were first mechanically polished and cut into 1cm × 2 cm samples. Then, the substrates were separately sonicated in acetone, isopropanol, and ethanol, each for 5 min, before being rinsed with deionized (DI) water. The anodization process was performed at 60 V for 2–6 hr using an electrolyte consisting of 0.25 wt % NH_4F and 0.75% H_2O in ethylene glycol. The anodized samples were rinsed with DI water and then soaked in methanol for 30 s to initiate the detachment procedure. Free-standing TNT membranes were separated from the Ti substrate by drying the methanol-wetted samples with a stream of N_2 gas. This caused the freshly formed TNT array to delaminate from the substrate. To effectively remove the TNT membranes, methanol wetting and N_2 blowing may need to be repeated several times. The Ti substrates from the first step were then anodized a second time using a fresh electrolyte solution of the same composition. The separation procedure was repeated in order to achieve highly ordered free-standing TiO_2 nanotube arrays with clear, open-top ends.

To crystallize the amorphous TNT arrays into the anatase phase, a two-step annealing process was used. First the TNT arrays were subjected to 200 °C for 1 hr using a ramp rate of 1 °C s^{-1}. The arrays were then further heated at 475 °C for 3 h using a heating rate of 30 °C s^{-1}. After annealment, the arrays are to be bonded to a PET film using a TiO_2 sol containing titanium butoxide and polyethylene glycol. The TNT/PET was then annealed at a low temperature of 200 °C.

Following the annealing process, the TNT/PET films are to be sensitized using a bacteriorhodopsin dye (bR) for 16 hr. To evaluate their performance, the dye-sensitized TNT/PET films will be closed together using an electrolyte and indium tin dioxide-coated PET.

3. Results and Discussion

Figure 5 shows the effects of methanol wetting and N_2 blowing on freshly anodized TNT arrays. Due to the low surface-tension of methanol, soaking the TNT arrays allows the methanol to penetrate the oxidized layer and aid in the delaminating of the nanotube layer. This resulted in a nanotube array nearly twice the size of one collected without methanol wetting.
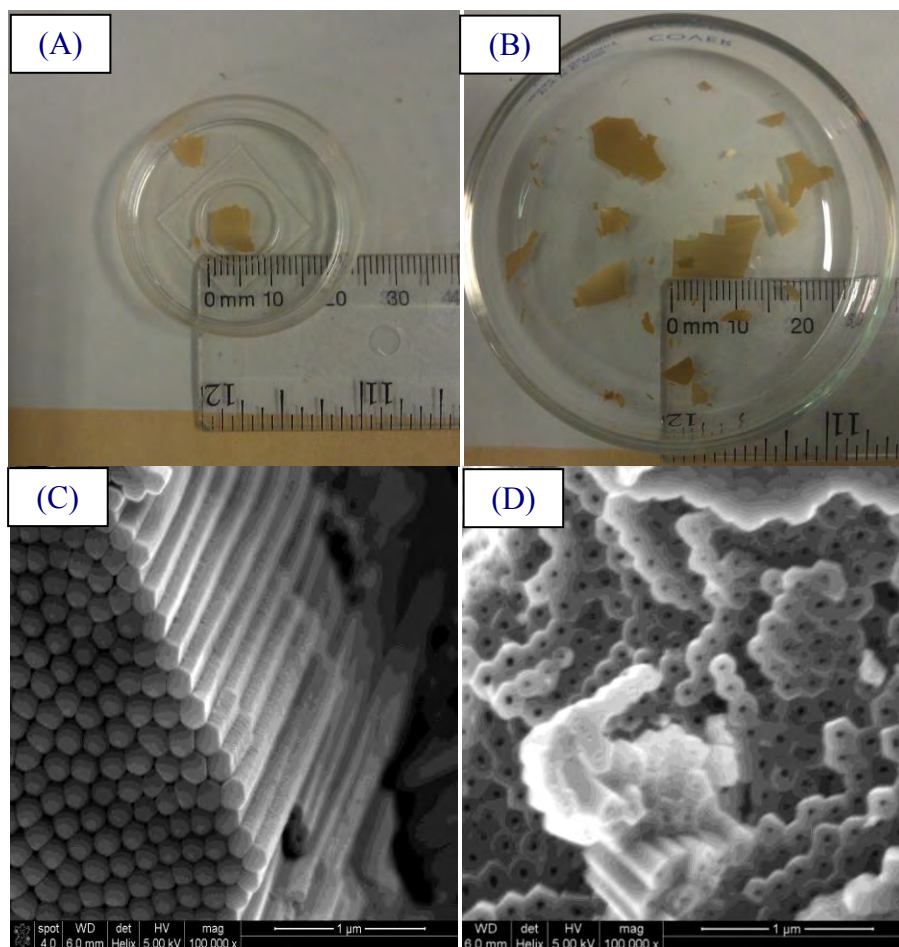

Figure 5. (a) Without methanol wetting, (b) with methanol wetting, (c) side SEM view of hexagonal, highly-oriented nanotube array, and (d) top view.

SEM images in figure 5 (c and d) show highly packed, hexagonally oriented nanotube arrays. This result was highly unexpected, because the arrays were formed using a single-step anodization procedure. These highly organized arrays were anodized at 60 V for 3 h, and had a length of 19 µm, tube thickness of 64 nm, and a pore diameter of 32 nm. The high wall thickness compared to pore size is most likely due to a low concentration of F^- ions in the electrolyte solution, which slowed down the dissolution rate, thus increasing the inner diameter. Since this was made immediately after mixing a batch of electrolyte solution (0.25 wt % NH_4F and 0.75%

H$_2$O in ethylene glycol), it is possible that the NH$_4$F was not equally distributed. The opposite affect can be seen in figure 6, in which the uneven distribution of NH$_4$F right after mixing a batch of electrolyte solution resulted in extraordinarily high concentration of F$^-$ and the complete dissolution of the titanium electrode.
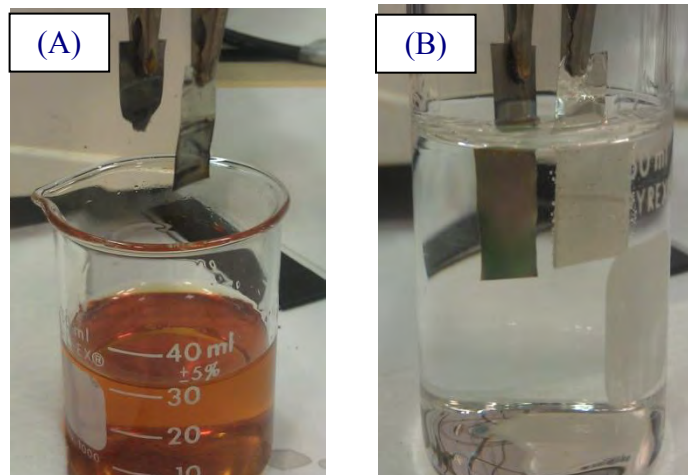

Figure 6. (a) Anodization with a high NH$_4$F Concentration and
(b) anodization with a normal NH$_4$F concentration.

Although SEM images of samples anodized using different solution concentrations are not shown here, the effects of a longer anodization time at the same voltage and concentration are demonstrated in figures 5 and 7. The SEM images report samples that were anodized for 6 h at 60 V, using the same solution as the samples shown in figure 5. However, it is clear that the results are drastically different. This shows the effects of electrode preparation, as well as the sensitivity of the nanotubes. The SEM images report grass-like structures, also known as nano-wires, of approximately 24 nm thickness sitting on top of a highly porous honeycomb-like nanostructure with wall thickness of only 36 nm. The "nano-grass" is most likely the result of not mechanically polishing and sonicating the electrode prior to anodization. This allowed the chemical attack on the tube ends and the formation of nanograss. The top surface was left non-uniform compared to that of figure 5, resulting in an uneven dissolution of the Ti. The longer anodization time presumably contributed the rapid breakdown of the nanotubes.
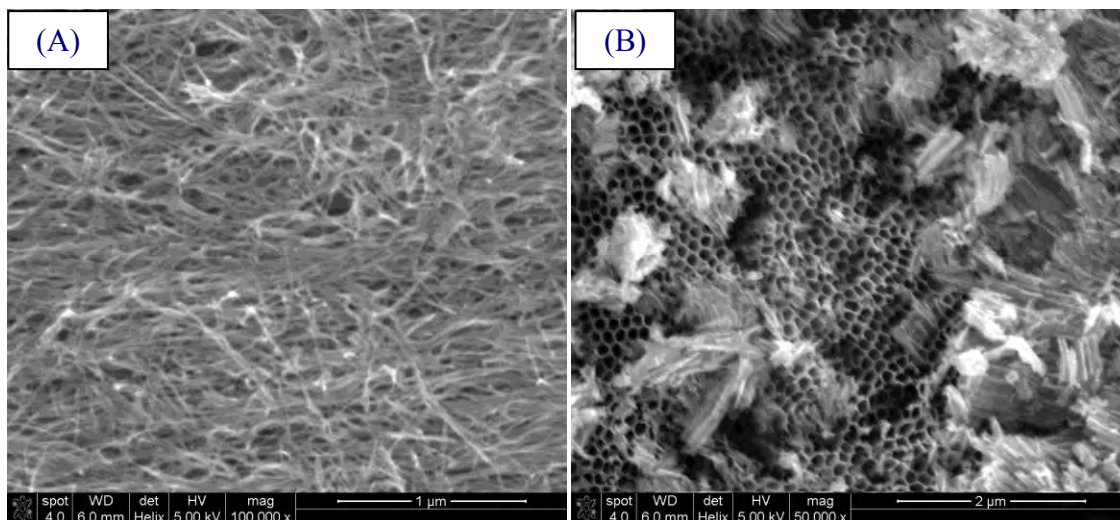
Figure 7. (a) Nanograss formations and (b) honey-comb structure.

4. Summary and Conclusions

This study presents a method of obtaining free-standing, highly organized TiO_2 arrays for use in flexible dye-sensitized solar cells. Free-standing, highly oriented, hexagonally packed nanotubes were made. Future efforts will be directed towards combining the nanotubes with an indium tin dioxide PET using a sol-gel consisting of Ti nanoparticles. In order to improve the reported results, a higher concentration of NH_4F should be used in the electrolyte solution. This will increase the inner diameter reported in figure 5, allowing for the use of a bR dye. An anodization time of less than 6 h should be used in order to avoid the dissolution at the nanotube tops into nanograss. Although the nanograss and honeycomb structures found in this study are not idea for use in a DSSC, they may have other valuable uses besides photovoltaics, such as bacteria filters and other biomedical applications.

5. References

1. Kang, M. G.; Park, N.-G.; Ryu, K. S.; Chang, S. H. 2001, p. 7.

2. Grätzel, M. *Inorg. Chem.* **2005**, *44*, 6841.

3. Jennings, J. R.; Ghicov, A. *J. Am. Chem. Soc.* **2008**, *130*, 13364–13372.

4. Chiba, Y.; Islam, A.; Watanabe, Y.; Komiya, R.; Koide, N.; Han, L. *Jpn. J. Appl. Phys.* **2006**, *45*, L638.

5. Koops, S. E.; O'Regan, B. C.; Barnes, P.R.F.; Durrant, J. R. *J. Am. Chem. Soc.* **2009**, *131*, 4808.

6. Nelson, J. *Phys. Rev. B: Condens. Matter Mater. Phys.* **1999**, *59*, 15374, LP.

7. Shankar, K.; Mor, G. K.; Prakasam, H. E.; Varghese, O.K.; Grimes, C. A. *Lamg,ior* **2007**, *23*, 12444–12449.

8. Zhu, K.; Neale, N. R.; Miedaner, A.; Frank, A. J. *Nano Lett.* **2007**, *7*, 69–74

9. Ghicov, Andrei; Albu, Sergiu. $Ti0_2$ Nanotubes in Dye-Sensitized Solar Cells: Critical Factors for the Conversion Efficiency. *Chem. Asian J.* **2009**, *4*, 520–525.

10. Elsanousi, A.; Zhang, J. Self-Organized $Ti0_2$ Nanotubes with controlled dimensions by anodic Oxidation. *J Mater Sci* **2008**, *43*, 7219–7729.

11. Cai, Q.; Paulose, M.; Varghese, O. K. *J Mater Res* **2005**, *20*, 230, doi: 10.1557/JMR.2005.0020.

12. Macak, J. M.; Taveroa, L. V.; Tsuchiya, H.; Sirotna, K.; Macak, J.; Schumuki, P. *J Electroceram, 16*, 29.

13. Mor, G. K.; Carvalho, M. A.; Varghese, O. K.; Pisho, M. V.; Grimes, C.A. *J Mater Sci* **2004**, *19*, 628.

14. Prakasam, H. E.; Shankar, K.; Paulose, M.; Varghese, O. K.; Grimes, C. A. A New Benchmark for $Ti0_2$ Nanotube Array Growth by Anodization. *J. Phys. Chem* **2007**, *111*, 7235–7241.

15. Lei, B.; Liao, J.; Zhang, R.; Wang, J.; Su, C.; Kuang, D. Ordered Crystalline $Ti0_2$ Nanotube Arrays on Transparent FTO Glass for Efficient Dye-Sensitized Solar Cells. *J. Phys. Chem. C* **2010**, *114*, 15528–33.

16. Park, N. G.; Frank, A. J. Comparison of Dye-Sensitized Rutile and Anatase-Based $Ti0_2$ Solar Cells. *J. Phys. Chem. B* **2000***, 104*, 8989–8994.

17. Yang, D. J.; Kim, H. G.; Cho, S. J.; Choi, W. Y. *Mater Lett* **2008**, *62*, 775, doi:10.1016/j.matlet.2007.06.058.

18. Macak, J. M.; Tsuchiya, H.; Ghicov, A.; Yashuda, K.; Schumuki, P. *Curr Opin Solid State Mater Sci* **2007**, *11*, 3, doi:10.1016/j.cossms.2007.08.004.